HAL open science

Advection and dispersion of bed load tracers

Eric Lajeunesse, Olivier Devauchelle, Francois James

To cite this version:

Eric Lajeunesse, Olivier Devauchelle, Francois James. Advection and dispersion of bed load tracers. Earth Surface Dynamics, 2018, 6 (2), pp.389-399. 10.5194/esurf-6-389-2018 . hal-01851929

HAL Id: hal-01851929

https://hal.science/hal-01851929

Submitted on 31 Jul 2018

HAL is a multi-disciplinary open access archive for the deposit and dissemination of scientific research documents, whether they are published or not. The documents may come from teaching and research institutions in France or abroad, or from public or private research centers.

L'archive ouverte pluridisciplinaire **HAL**, est destinée au dépôt et à la diffusion de documents scientifiques de niveau recherche, publiés ou non, émanant des établissements d'enseignement et de recherche français ou étrangers, des laboratoires publics ou privés.

Earth Surf. Dynam., 6, 389–399, 2018
https://doi.org/10.5194/esurf-6-389-2018
© Author(s) 2018. This work is distributed under
the Creative Commons Attribution 4.0 License.

Earth Surface Dynamics
Open Access
EGU

Advection and dispersion of bed load tracers

Eric Lajeunesse[1], **Olivier Devauchelle**[1], **and François James**[2]

[1]Institut de Physique du Globe de Paris – Sorbonne Paris Cité, Équipe de Dynamique des Fuides Géologiques, 1 rue Jussieu, 75238 Paris CEDEX 05, France
[2]Institut Denis Poisson, Université d'Orléans, Universitéde Tours, CNRS, Route de Chartres, BP 6759, 45067 Orléans CEDEX 2, France

Correspondence: E. Lajeunesse (lajeunes@ipgp.fr)

Received: 14 September 2017 – Discussion started: 9 November 2017
Revised: 5 March 2018 – Accepted: 16 April 2018 – Published: 15 May 2018

Abstract. We use the erosion–deposition model introduced by Charru et al. (2004) to numerically simulate the evolution of a plume of bed load tracers entrained by a steady flow. In this model, the propagation of the plume results from the stochastic exchange of particles between the bed and the bed load layer. We find a transition between two asymptotic regimes. The tracers, initially at rest, are gradually set into motion by the flow. During this entrainment regime, the plume is strongly skewed in the direction of propagation and continuously accelerates while spreading nonlinearly. With time, the skewness of the plume eventually reaches a maximum value before decreasing. This marks the transition to an advection–diffusion regime in which the plume becomes increasingly symmetrical, spreads linearly, and advances at constant velocity. We analytically derive the expressions of the position, the variance, and the skewness of the plume and investigate their asymptotic regimes. Our model assumes steady state. In the field, however, bed load transport is intermittent. We show that the asymptotic regimes become insensitive to this intermittency when expressed in terms of the distance traveled by the plume. If this finding applies to the field, it might provide an estimate for the average bed load transport rate.

1 Introduction

Alluvial rivers transport the sediment that makes up their bed. From a mechanical standpoint, the flow of water applies a shear stress on the sediment particles and entrains some of them downstream. When the shear stress is weak, the particles remain close to the bed surface as they travel (Shields, 1936). They roll, slide, and bounce over the rough bed until they settle down (Fernandez-Luque and Van Beek, 1976; Van Rijn, 1984; Nino and Garcia, 1994). This process is called bed load transport.

Bed load transport is inherently random (Einstein, 1937). A turbulent burst or a collision with an entrained grain sometime dislodges a resting particle. The likeliness of this event depends on the specific arrangement of the surrounding particles. On average, however, the probability of entrainment is a function of macroscopic quantities such as shear stress and grain size (Ancey et al., 2008). Once dislodged, the velocity of a particle fluctuates significantly around its average (Lajeunesse et al., 2010a; Furbish et al., 2012b, c, a; Roseberry et al., 2012). Finally, the particle's return to rest is yet another random event. Overall, a bed load particle spends only a small fraction of its time in motion.

Altogether, the combination of these stochastic processes results in a downstream flux of particles. Fluvial geomorphologists measure this flux by collecting moving particles in traps or Helley–Smith samplers (Leopold and Emmett, 1976; Helley and Smith, 1971). The instantaneous sediment discharge fluctuates due to the inherent randomness of bed load transport. However, averaging measurements over time yields a consistent sediment flux (Liu et al., 2008).

An alternative approach to sediment flux measurements is to follow the fate of tracer particles. In November 1960, Sayre and Hubbell (1965) deposited 18 kg of radioactive sand in the North Loup River, a sand-bed stream located in Nebraska (USA). Using a scintillator detector, they observed that the plume of radioactive sand gradually spread as it was entrained downstream. Tracking cobbles in gravel-

bed rivers reveals a similar behavior: tracers disperse as they travel downstream (Bradley et al., 2010; Bradley and Tucker, 2012; Hassan et al., 2013; Phillips et al., 2013).

The dispersion of the tracers, expressed as the variance of their location, results from the randomness of bed load transport. Nikora et al. (2002) identify three regimes with distinct timescales. A particle entrained by the flow repeatedly collides with the bed (Lajeunesse et al., 2017). At short timescales, i.e., between two collisions, particles move with the flow, and the variance increases as the square of time (Martin et al., 2012; Fathel et al., 2016). This regime is analogous to the ballistic regime of Brownian motion (Zhang et al., 2012; Fathel et al., 2016).

As the particle continues its course, collisions deviate its trajectory. In this intermediate regime, the variance increases nonlinearly with time (Martin et al., 2012). Nikora et al. (2002) attribute this behavior to anomalous super-diffusion, but Fathel et al. (2016) contest their interpretation.

With time, tracers settle back on the bed, where they can remain trapped for a long time. How the distribution of resting times influences the long-term dispersion of tracers remains unknown. The data collected by Sayre and Hubbell (1965) are consistent with the existence of a diffusive regime in which the variance increases linearly (Zhang et al., 2012). Other investigators, however, report either sub-diffusion or super-diffusion (Nikora et al., 2002; Bradley, 2017). These anomalous diffusion regimes are sometimes modeled with fractional advection–dispersion equations (Schumer et al., 2009; Ganti et al., 2010; Bradley et al., 2010).

The variability of the stream discharge further complicates the interpretation of field data. Bed load transport occurs when the shear stress exceeds a threshold set by the grain size. Most rivers fulfill this condition only a small fraction of the time, making sediment transport highly intermittent (Phillips et al., 2013; Phillips and Jerolmack, 2014). The rate at which tracers spread thus depends not only on the inherent randomness of bed load transport, but also on the probability distribution of the river discharge (Ganti et al., 2010; Phillips et al., 2013; Bradley, 2017).

Laboratory experiments under well-controlled conditions isolate these two effects. For instance, Lajeunesse et al. (2017) tracked a plume of dyed particles in an experimental channel. Although the flow was constant in this experiment, the tracers still dispersed as they traveled downstream. In this case, dispersion resulted from the inherent randomness of bed load transport only. We can decompose this randomness into two components. First, the velocity fluctuations disperse the particles (Furbish et al., 2012a, c, 2017). Secondly, the random exchange of particles between the bed load layer, where particles travel, and the sediment bed, where particles are at rest, further disperses the particles (Lajeunesse et al., 2013, 2017). This effective diffusion also occurs in chromatography experiments in which a bonded phase exchanges the analyte with the flow (Van Genuchten and Wierenga, 1976).

In a recent paper, Lajeunesse et al. (2013) used the erosion–deposition model introduced by Charru et al. (2004) to derive the equations governing the evolution of a plume of tracers. Neglecting velocity fluctuations, they found that the second dispersion process, namely the exchange of particles between the bed load layer and the sediment bed, efficiently disperses the tracers. They also observed the transition between an initial transient and classical advection–diffusion. In the present paper, we further this investigation. Our objective is to formally derive the contribution of the advection exchange of particles to the dispersion of a plume of tracers. To do so, we briefly rederive the equations governing the evolution of a plume of tracers (Sect. 2). We numerically simulate the propagation of a plume of tracers and discuss the nature of the two asymptotic regimes evidenced in Lajeunesse et al. (2013) (Sect. 3). We analyze the long-time advection–diffusion behavior of the plume and provide an analytical expression for the diffusion coefficient and the plume velocity (Sect. 4). We analytically derive the mean, the variance, and the skewness of the tracer distribution and describe their asymptotic behavior in each regime (Sect. 5). Finally, we discuss the applicability of these results to the field (Sect. 6).

2 Entrainment of tracers

In most rivers, sediment is broadly distributed in size. This likely influences the dispersion of bed load tracers (Martin et al., 2012; Houssais and Lajeunesse, 2012; Pelosi et al., 2014). For the sake of simplicity, however, we restrict our analysis to a bed of uniform particles of size d_s. The bed is sheared by a flow, which applies a shear stress strong enough to entrain some particles. The latter remain confined in a thin bed load layer.

For moderate values of the shear stress, the concentration of moving sediments is small, and we can neglect the interactions between particles. The erosion–deposition model introduced by Charru et al. (2004) provides an accurate description of this dilute regime in which bed load transport is controlled by the exchange of particles between the sediment bed and the bed load layer. This exchange sets the surface concentration of moving particles, n_m, through mass balance:

$$\frac{\partial n_\mathrm{m}}{\partial t} + V\,\frac{\partial n_\mathrm{m}}{\partial x} = E - D, \tag{1}$$

where we introduce the average particle velocity V. E is the erosion rate, defined as the number of bed particles set in motion per unit of time and area. Similarly, the deposition rate D is defined as the number of bed load particles settling on the bed per unit of time and area (Charru et al., 2004; Charru, 2006; Lajeunesse et al., 2010b; Seizilles et al., 2014; Lajeunesse et al., 2017).

To investigate the dispersion of bed load particles, we consider some of them to be marked (Fig. 1). We refer to these marked particles as "tracers" and assume that their physical properties are the same as those of unmarked particles. With

these assumptions, the mass balance for the tracers in the bed load layer reads

$$n_{\mathrm{m}}\frac{\partial\phi}{\partial t}+n_{\mathrm{m}}V\frac{\partial\phi}{\partial x}=E\psi-D\phi, \tag{2}$$

where we introduce the proportion of tracers in the moving layer, ϕ. Similarly, ψ is the proportion of tracers on the bed surface.

When subjected to varying flow and sediment discharges, the bed of a stream accumulates or releases sediments (Gintz et al., 1996; Blom and Parker, 2004). Some particles may then be temporary buried within the bed, inducing streamwise dispersion (Crickmore and Lean, 1962; Pelosi et al., 2014). Here, we neglect this mechanism and restrict our analysis to steady and uniform sediment transport. Accordingly, we assume that erosion and deposition affects the bed over a depth of about one grain diameter only. This hypothesis holds if the departure from the entrainment threshold is small enough. With these assumptions, the mass balance for the tracers on the bed surface reads

$$n_{\mathrm{s}}\frac{\partial\psi}{\partial t}=D\phi-E\psi, \tag{3}$$

where n_{s} is the surface concentration of particles at rest on the bed surface. Each of them occupies an area of about d_{s}^2. The surface concentration of particles at rest is therefore $n_{\mathrm{s}}\sim 1/d_{\mathrm{s}}^2$.

For steady and uniform transport, the surface concentration of moving particles, n, is constant. In addition, erosion and deposition balance each other:

$$E=D. \tag{4}$$

Laboratory experiments suggest that the deposition rate is proportional to the concentration of moving particles:

$$D=\frac{n_{\mathrm{m}}}{\tau_{\mathrm{f}}} \tag{5}$$

where we introduce the average flight duration, $\tau_{\mathrm{f}}=\ell_{\mathrm{f}}/V$, and the average flight length, ℓ_{f} (Charru et al., 2004; Lajeunesse et al., 2010b). The flight length is the distance traveled by a mobile particle between its erosion and eventual deposition. Similarly, the flight duration is the time a particle spends in the bed load layer. In practice, measuring these quantities often proves difficult, since they depend on how one defines the mobile and the static layer (Lajeunesse et al., 2017).

Combining Eq. (2), (3), (4), and (5) provides the set of equations that describe the propagation of the plume:

$$\frac{\partial\phi}{\partial t}+V\frac{\partial\phi}{\partial x}=\frac{1}{\tau_{\mathrm{f}}}(\psi-\phi), \tag{6}$$

$$\frac{\partial\psi}{\partial t}=-\frac{\alpha}{\tau_{\mathrm{f}}}(\psi-\phi), \tag{7}$$

where we define $\alpha=n_{\mathrm{m}}/n_{\mathrm{s}}\sim n_{\mathrm{m}}d_{\mathrm{s}}^2$, the ratio of the concentration of moving particles to the concentration of static particles. This ratio is smaller than 1. It is proportional to the intensity q_{s} of bed load transport:

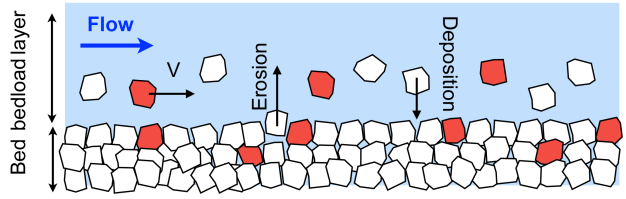

Figure 1. Granular bed sheared by a steady and uniform flow. The bed is a mixture of marked (red) and unmarked (white) grains.

$$\alpha\sim\frac{d_{\mathrm{s}}^2}{V}q_{\mathrm{s}}. \tag{8}$$

Complemented with initial and boundary conditions, Eqs. (6) and (7) describe the evolution of the plume. In dimensionless form, they read

$$\frac{\partial\phi}{\partial\hat{t}}+\frac{\partial\phi}{\partial\hat{x}}=\psi-\phi, \tag{9}$$

$$\frac{\partial\psi}{\partial\hat{t}}=-\alpha(\psi-\phi), \tag{10}$$

where $\hat{t}=t/\tau_{\mathrm{f}}$ and $\hat{x}=x/\ell_{\mathrm{f}}$ are dimensionless variables. For ease of notation, we drop the hat symbol in what follows.

A single parameter controls Eqs. (9) and (10): the ratio of surface densities α, which characterizes the average distance between grains in the bed load layer. Since the erosion–deposition model assumes independent particles, we can only expect it to be valid when moving particles are sufficiently far away from each other, which is when α is small or, equivalently, when the Shields parameter is near the threshold.

In the next section, we numerically solve Eqs. (9) and (10).

3 Propagation of a plume of tracers

Laboratory measurements of bed load often use top-view images (Martin et al., 2012; Lajeunesse et al., 2017). Unless individual particles can be tracked, the tracers at rest are usually indistinguishable from those entrained by the flow. Separating the proportion of tracers in the moving layer, ϕ, from that on the bed surface, ψ, is practically impossible. Instead, top-view pictures show the total concentration of tracers:

$$c=\frac{n_{\mathrm{m}}\phi+n_{\mathrm{s}}\psi}{n_{\mathrm{m}}+n_{\mathrm{s}}}=\frac{\alpha}{\alpha+1}\phi+\frac{1}{\alpha+1}\psi. \tag{11}$$

Tracking sediment in rivers poses a similar problem. In general, one records the position of the tracers when the river stage is below the threshold of grain entrainment (Phillips et al., 2013; Phillips and Jerolmack, 2014). At the time of measurement, all tracers are therefore at rest. As a result, the

proportion of mobile tracers vanishes ($\phi = 0$), and the total concentration of tracers reads $c = \psi/(\alpha + 1)$.

In summary, the proportions of mobile and static tracers, ϕ and ψ, naturally derive from mass balance (Eq. 2) and Eq. (3). However, their measurement proves difficult during active transport. On the other hand, experimental and field investigations provide the total concentration of tracers, c (Sayre and Hubbell, 1965; Lajeunesse et al., 2017). This quantity is conservative, as the total amount of tracers, $M = \int c\,\mathrm{d}x$, is preserved. In the following, we therefore focus on the concentration of tracers, c.

To study the evolution of the tracer concentration, we solve Eqs. (9) and (10) numerically using a finite-volume scheme. We then compute the tracer concentration using Eq. (11) (Fig. 2).

The early evolution of the plume depends on initial conditions. In most field experiments, tracers are deposited at the surface of the river bed when the flow stage is low and sediment is motionless (Phillips et al., 2013). During floods, the river discharge increases and the shear stress eventually exceeds the entrainment threshold, setting in motion some of the grains. The entrainment of particles strongly depends on the arrangement of the bed: grains highly exposed to the flow move first (Charru et al., 2004; Turowski et al., 2011; Agudo and Wierschem, 2012). Several authors find that the tracers they disposed on the bed are more mobile during the first flood than during later ones (Bradley and Tucker, 2012). During the later floods, tracers gradually get trapped in the bed, and their average mobility decreases. On the other hand, Phillips and Jerolmack (2014) find no special mobility during the first flood. In the absence of a clear scenario, we choose the simplest possible initial conditions and assume that initially all tracers belong to the static layer: $\phi(x, t = 0) = 0$.

With these initial conditions, the evolution of the plume follows two distinct regimes. At early times, the flow gradually dislodges tracers from the bed and entrains them in the bed load layer. During this entrainment regime, only a small proportion of the tracers move. Consequently, the plume develops a thin tail in the downstream direction (Fig. 2a). The corresponding distribution of travel distances is strongly skewed towards the direction of propagation, a feature commonly observed in field experiments (Liébault et al., 2012; Phillips and Jerolmack, 2014).

With time, the plume moves downstream and spreads both upstream and downstream. As a result, the concentration rapidly decreases to small levels. The plume becomes gradually symmetrical and tends asymptotically towards a Gaussian distribution (Fig. 2b). This regime is reminiscent of classical diffusion.

To better illustrate this evolution, we introduce the mean position of the plume of tracers:

$$\langle x \rangle = \frac{1}{M} \int_{-\infty}^{\infty} c x \mathrm{d}x. \tag{12}$$

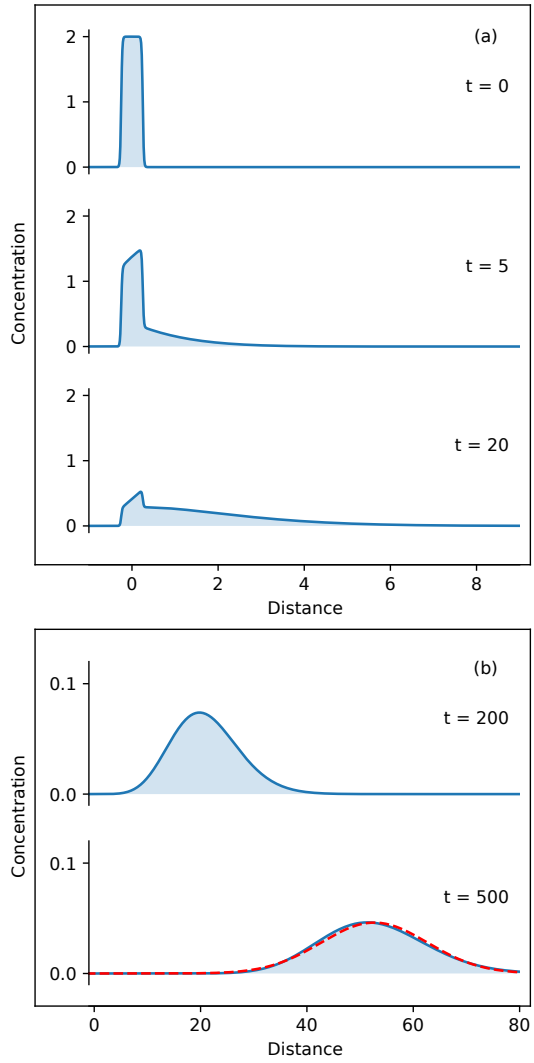

Figure 2. Evolution of the tracer concentration ($\alpha = 0.1$) obtained by numerically solving Eqs. (9) and (10). **(a)** Early entrainment regime. **(b)** Relaxation towards the diffusive regime. Tracers are initially at rest, forming a symmetric plume of length $L = 0.5$ and mass $M = 1$. The concentration profile asymptotically tends towards a Gaussian distribution (dotted red line).

We also characterize its size with the variance,

$$\sigma^2 = \frac{1}{M} \int_{-\infty}^{\infty} c(x - \langle x \rangle)^2 \mathrm{d}x, \tag{13}$$

and its symmetry with the skewness,

$$\gamma = \frac{1}{M} \int_{-\infty}^{\infty} c \left(\frac{x - \langle x \rangle}{\sigma} \right)^3 \mathrm{d}x. \tag{14}$$

The evolution of these three moments is consistent with the existence of two asymptotic regimes (Fig. 3). At short

timescales, the plume grows a thin tail downstream. This deformation causes the plume's skewness to increase as t^4. During this regime, the average location of the plume increases as t^2 and its variance grows as t^3. Although the variance increases nonlinearly with time, the exponent, 3, is too large for super-diffusion (Weeks and Swinney, 1998).

After a characteristic time of the order of $\tau \approx \tau_f$, the skewness of the plume reaches a maximum (Fig. 3c). This corresponds to a drastic change in dynamics: the skewness starts decreasing as the plume becomes gradually more symmetrical. At long timescales, the plume of tracers advances at constant velocity and diffuses linearly with time (Fig. 3a and b). This regime, regardless of the value of α, corresponds to classical advection–diffusion.

Next, we establish the equivalence between diffusion and the long-time behavior of the tracers.

4 Advection–diffusion at long timescales

The diffusion at work in Eqs. (9) and (10) results from the continuous exchange of particles between the bed load layer, where particles travel at the constant velocity V, and the sediment bed, where particles are at rest. The velocity difference between the two layers gradually smears out the plume and spreads it in the flow direction. This process occurs in a variety of physical systems in which layers moving at different velocities exchange a passive tracer. A typical example is Taylor dispersion, whereby a passive tracer diffuses across a Poiseuille flow in a circular pipe (Taylor, 1953). The combination of shear rate and transverse molecular diffusion generates an effective diffusion in the flow direction. Other examples of effective diffusion include solute transport in porous media and chromatography (Van Genuchten and Wierenga, 1976).

To formally establish the equivalence between diffusion and the long-time behavior of the plume, we follow a reasoning similar to the one developed for chromatography (James et al., 2000). Equations (9) and (10) are equivalent to

$$\frac{\partial c}{\partial t} + \frac{\alpha}{\alpha+1}\frac{\partial c}{\partial x} = \frac{\alpha}{(\alpha+1)^2}\frac{\partial \delta}{\partial x}, \tag{15}$$

$$\frac{\partial \delta}{\partial t} + \frac{1}{\alpha+1}\frac{\partial \delta}{\partial x} + (\alpha+1)\delta = \frac{\partial c}{\partial x}, \tag{16}$$

where we introduce $\delta = \psi - \phi$, the difference between the proportion of tracers on the sediment bed and that in the bed load layer. Eventually, these proportions equilibrate each other. At long timescales, we therefore expect the solution to Eqs. (15) and (16) to relax towards steady state, for which δ is of order $\epsilon \ll 1$. Accordingly, we rewrite these two equations as

$$\frac{\partial c}{\partial t} + \frac{\alpha}{\alpha+1}\frac{\partial c}{\partial x} = \epsilon\frac{\alpha}{(\alpha+1)^2}\frac{\partial \delta}{\partial x}, \tag{17}$$

$$\frac{\partial \delta}{\partial t} + \frac{1}{\alpha+1}\frac{\partial \delta}{\partial x} + (\alpha+1)\delta = \frac{1}{\epsilon}\frac{\partial c}{\partial x}. \tag{18}$$

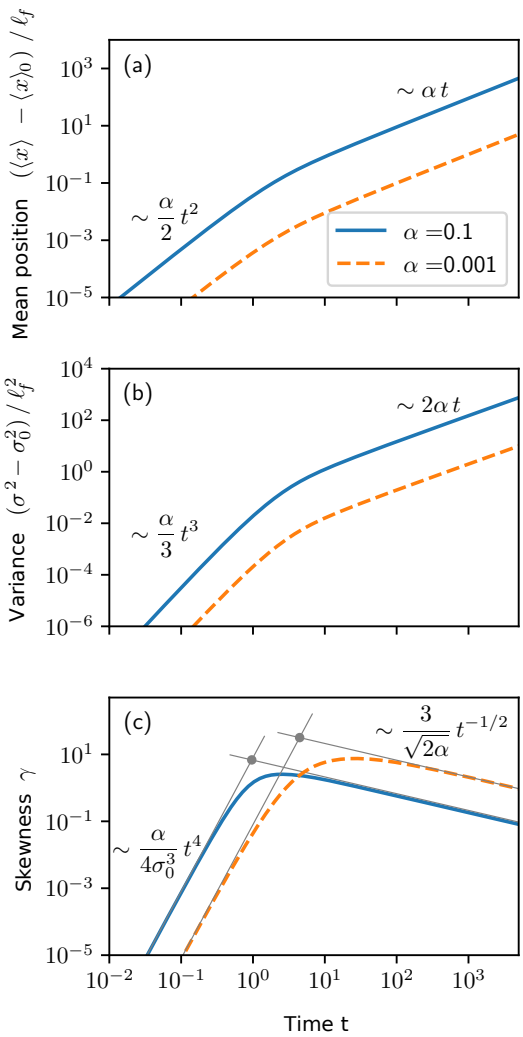

Figure 3. **(a)** Position, **(b)** variance, and **(c)** skewness of a plume of tracers as a function of time for $\alpha = 0.1$ and $\alpha = 0.001$. We compute the evolution of these three quantities using Eqs. (28), (33), and (38). The results agree exactly with numerical simulations. The asymptotic regimes of the skewness are represented with grey lines. Their intersection provides an estimate of the duration of the entrainment regime (see Eq. 45).

Introducing $T = \epsilon t$ and $X = \epsilon x$ and developing c and δ with respect to ϵ yields

$$\frac{\partial c_0}{\partial T} + \frac{\alpha}{\alpha+1}\frac{\partial c_0}{\partial X} = 0 \tag{19}$$

$$(\alpha+1)\delta_0 = \frac{\partial c_0}{\partial X} \tag{20}$$

at zeroth order and

$$\frac{\partial c_1}{\partial T} + \frac{\alpha}{\alpha+1}\frac{\partial c_1}{\partial X} = \frac{\alpha}{(\alpha+1)^2}\frac{\partial \delta_0}{\partial X} \tag{21}$$

at first order.

By multiplying Eq. (21) by ϵ and summing the result with Eq. (19), we finally get

$$\frac{\partial c}{\partial t}+\frac{\alpha}{\alpha+1}\frac{\partial c}{\partial x}=\frac{\alpha}{(\alpha+1)^3}\frac{\partial^2 c}{\partial x^2}. \tag{22}$$

At long timescales, the transport of the tracers follows the advection–diffusion equation (Eq. 22). We identify the advection velocity, U, which reads

$$U=\frac{\alpha}{\alpha+1}\frac{\ell_\mathrm{f}}{\tau_\mathrm{f}}\sim\alpha\frac{\ell_\mathrm{f}}{\tau_\mathrm{f}}. \tag{23}$$

Likewise, the diffusion coefficient reads

$$C_\mathrm{d}=\frac{\alpha}{(\alpha+1)^3}\frac{\ell_\mathrm{f}^2}{\tau_\mathrm{f}}\sim\alpha\frac{\ell_\mathrm{f}^2}{\tau_\mathrm{f}}. \tag{24}$$

This asymptotic equivalence explains the advection–diffusion regime (Figs. 2 and 3).

We interpret this formal derivation as follows. In the reference frame of the plume, a tracer at rest on the bed moves backward, while a tracer entrained in the bed load layer moves forward. At long timescales, the proportions of tracers in each layer equilibrate. Consequently, the probability that a tracer will be entrained and move forward equals that of deposition. In the reference frame of the plume, the exchange of particles between the bed and the bed load layer is thus a Brownian motion driving the linear diffusion of the plume.

In the next section, we investigate the evolution of the location, the size, and the symmetry of the plume as it propagates downstream.

5 Location, size, and symmetry of the plume

Concentration, defined as the number of tracers per unit of area, depends on the area over which it is measured. Its value is meaningful when the measurement area is much larger than the distance between particles and much smaller than the plume. During the entrainment regime, the plume develops a thin tail containing only a small proportion of tracers. Measuring the concentration profile during this regime is thus challenging. To our knowledge, only Sayre and Hubbell (1965) were able to measure consistent concentration profiles using radioactive sand. In practice, most field campaigns involve a limited number of tracers (900 at most) (Liébault et al., 2012; Bradley and Tucker, 2012; Phillips and Jerolmack, 2014; Bradley, 2017). It is thus more practical to consider integral quantities, such as the mean position of the plume $\langle x\rangle$, its variance σ^2, and its skewness γ.

Multiplying Eq. (15) by x and integrating over space provides the evolution equation for the mean position:

$$\frac{\partial\langle x\rangle}{\partial t}=\frac{\alpha}{\alpha+1}-\frac{\alpha}{(\alpha+1)^2}\langle\delta\rangle, \tag{25}$$

where

$$\langle\delta\rangle=\frac{1}{M}\int\delta\,\mathrm{d}x \tag{26}$$

is the average difference between the proportion of tracers on the sediment bed and in the bed load layer. To solve Eq. (25), we need an equation for $\langle\delta\rangle$. The latter is obtained by integrating Eq. (16) over space:

$$\frac{\partial\langle\delta\rangle}{\partial t}=-(\alpha+1)\langle\delta\rangle. \tag{27}$$

Equations (25) and (27) describe the downstream motion $\langle x\rangle$ of the plume. To solve them, we need to specify initial conditions. As discussed in Sect. 3, we consider all tracers to initially belong to the static layer, i.e., $\phi(x,\,t=0)=0$. This condition and the conservation of mass, $\langle c\rangle=1$, provide initial conditions for $\langle\delta\rangle$: $\langle\delta\rangle(t=0)=\alpha+1$. With this condition, Eqs. (25) and (27) integrate into

$$\langle x\rangle-\langle x\rangle_0=\frac{\alpha}{\alpha+1}t+\frac{\alpha}{(\alpha+1)^2}\left(e^{-(\alpha+1)t}-1\right), \tag{28}$$

where $\langle x\rangle_0$ is the initial position of the plume.

We now focus on the variance of the plume. Multiplying Eq. (15) by x^2 and integrating over space yields the evolution equation for the second moment of the tracer distribution:

$$\frac{\partial\langle x^2\rangle}{\partial t}=\frac{2\alpha}{(\alpha+1)}\langle x\rangle-\frac{2\alpha}{(\alpha+1)^2}\langle x\delta\rangle, \tag{29}$$

where

$$\langle x\delta\rangle=\frac{1}{M}\int x\delta\,\mathrm{d}x \tag{30}$$

is the first moment of δ. To solve Eq. (29), we need an equation for this intermediate quantity. We obtain it by multiplying Eq. (16) by x and integrating over space:

$$\frac{\partial\langle x\delta\rangle}{\partial t}=-1-(\alpha+1)\langle x\delta\rangle+\frac{\langle\delta\rangle}{\alpha+1}. \tag{31}$$

At time $t=0$, $\langle x\delta\rangle(t=0)=(\alpha+1)\langle x\rangle_0$. Equations (29) and (31) with this initial condition provide the expression of the second moment of the tracer distribution:

$$\langle x^2\rangle=\langle x^2\rangle_0+\frac{2\alpha}{(\alpha+1)^3}\left(t+\frac{2-\alpha}{\alpha+1}\right)e^{-(\alpha+1)t}+\frac{\alpha^2}{(\alpha+1)^2}t^2+\frac{2\alpha(1-\alpha)}{(\alpha+1)^3}t+\frac{2\alpha(\alpha-2)}{(\alpha+1)^4}, \tag{32}$$

where $\langle x^2\rangle_0$ is the initial value of the second moment of the tracer distribution. We then deduce the variance of the plume from

$$\sigma^2=\langle x^2\rangle-\langle x\rangle^2. \tag{33}$$

We follow a similar procedure to derive the skewness of the plume. Multiplying Eq. (15) by x^3 and integrating over space yields the evolution equation for the third moment of the tracer distribution:

$$\frac{\partial\langle x^3\rangle}{\partial t}=\frac{3\alpha}{(\alpha+1)}\langle x^2\rangle-\frac{3\alpha}{(\alpha+1)^2}\langle x^2\delta\rangle, \tag{34}$$

where

$$\langle x^2\delta\rangle = \frac{1}{M}\int x^2\delta \mathrm{d}x \tag{35}$$

is the second moment of δ. Multiplying Eq. (16) by x^2 and integrating over space provides the evolution equation for this intermediate quantity:

$$\frac{\partial\langle x^2\delta\rangle}{\partial t} = -(\alpha+1)\langle x^2\delta\rangle + \frac{2}{\alpha+1}\langle x\delta\rangle - 2\langle x\rangle. \tag{36}$$

At time $t=0$, $\langle x^2\delta\rangle = (\alpha+1)\langle x^2\rangle_0$ and $\langle x^3\rangle = 0$. With these initial conditions, Eqs. (34) and (36) provide the expression of $\langle x^3\rangle$:

$$\begin{aligned}\langle x^3\rangle = {} & \frac{3\alpha}{\alpha+1}\left(\sigma_0^2 + \frac{2\alpha^2-8\alpha+2}{(\alpha+1)^4}\right)t \\ & + \frac{3\alpha}{(\alpha+1)^2}\left(\sigma_0^2 + \frac{2\alpha^2-12\alpha+6}{(\alpha+1)^4}\right)\left(e^{-(\alpha+1)t}-1\right) \\ & + \frac{3\alpha}{(\alpha+1)^4}\left(t - 4\frac{\alpha-1}{\alpha+1}\right)te^{-(\alpha+1)t} \\ & + \frac{\alpha^3}{(\alpha+1)^3}\left(t - \frac{3(\alpha-2)}{\alpha(\alpha+1)}\right)t^2\end{aligned} \tag{37}$$

from which we deduce the skewness of the plume as

$$\gamma = \frac{\langle x^3\rangle - 3\langle x\rangle\sigma^2 - \langle x\rangle^3}{\sigma^3}. \tag{38}$$

Equations (28), (32), (33), (37), and (38) represent the evolution of the mean, the variance, and the skewness of the tracer distribution. They describe the migration, spreading, and symmetry of the plume. They do not require any assumption other than the ones of the model itself and agree exactly with numerical simulations (Fig. 3).

As discussed in Sect. 3, numerical simulations reveal a transient during which the tracers, initially at rest, are gradually set into motion by the flow (Fig. 3). During this entrainment regime, the plume continuously accelerates, spreads nonlinearly, and becomes increasingly asymmetrical. To characterize this regime, we expand Eqs. (28), (32), (33), (37), and (38) to leading order in time:

$$\langle x\rangle - \langle x\rangle_0 \sim \frac{\alpha}{2}t^2, \tag{39}$$

$$\sigma^2 - \sigma_0^2 \sim \frac{\alpha}{3}t^3, \tag{40}$$

$$\gamma \sim \frac{\alpha}{4\sigma_0^3}t^4. \tag{41}$$

These three equations are consistent with our numerical simulations (Fig. 3).

Anomalous diffusion arises from heavy-tailed distributions of either the step length or the waiting time (Weeks and Swinney, 1998). The erosion–deposition model contains no such ingredient. Here the fast increase in the variance results from the exchange of particles between the sediment bed and the bed load layer at the beginning of the experiment. Over a time shorter than the flight duration τ_f, the tracers entrained by the flow do not settle back on the bed. They form a thin tail, which leaves the main body of the plume and moves downstream at the average particle velocity V (Fig. 2a). The plume therefore consists of a main body of virtually constant concentration, followed by a thin tail of length $\propto Vt$. Accordingly, we can split the integral that defines its mean position, Eq. (12), into two terms. The first one, obtained by integrating cx over the main body of the plume, yields the initial position of the plume $\langle x\rangle_0$. The second one, obtained by integrating cx over a tail of length Vt, scales as t^2. Summing these contributions yields Eq. (39). Similar reasonings yield Eqs. (40) and (41) for the variance and the skewness.

With time, the plume enters the diffusive regime. Its velocity and its spreading rate relax towards constants while its skewness decreases (Fig. 3). We derive the corresponding asymptotic behavior by expanding Eqs. (28), (32), (33), (37), and (38) in the limit of time being large:

$$\langle x\rangle - \langle x\rangle_0 \sim \frac{\alpha}{\alpha+1}t \sim \alpha t \tag{42}$$

$$\sigma^2 - \sigma_0^2 \sim 2\frac{\alpha}{(\alpha+1)^3}t \sim 2\alpha t \tag{43}$$

$$\gamma \sim \frac{3}{\sqrt{2\alpha}}\frac{1}{\sqrt{t}}. \tag{44}$$

The asymptotic regimes (Eqs. 42 and 43) are consistent with the expressions derived in Sect. 4.

The transition between the entrainment and the diffusive regime occurs when the skewness reaches its maximum value. Equating the skewness estimated from Eqs. (41) and (44) provides the approximate duration of the entrainment regime, τ. We find

$$\tau_\mathrm{e} = (72)^{1/9}\left(\frac{\sigma_0^2}{\alpha}\right)^{1/3}\tau_\mathrm{f}, \tag{45}$$

which compares well with our numerical simulations (Fig. 3). The duration of the entrainment regime increases with the initial size of the plume and decreases with the intensity of sediment transport.

The asymptotic regimes (Eqs. 39, 40, 41, 42, 43, and 44) assume that sediment transport is in steady state. In the next section, we discuss the intermittency of bed load transport in natural streams.

6 Intermittency of bed load transport

Our description of the plume of tracers is based on the assumption that sediment transport is in steady state. This hypothesis is often satisfied in laboratory flumes (Lajeunesse et al., 2017). In a river, it may be met for up to a few days

(Sayre and Hubbell, 1965). At longer timescales, however, most rivers alternate between low-flow stages during which sediment is immobile and floods during which bed particles are entrained downstream (Phillips and Jerolmack, 2016). Bed load transport is thus intermittent.

The intermittency of bed load transport influences the propagation of tracers in several ways. First of all, sediment transport during a flood modifies the structure of the bed (Lenzi et al., 2004; Turowski et al., 2009, 2011). As a result, the proportion of tracers in the bed load layer and in the bed, ϕ and ψ, likely change from one flood to the next. In a effort to address this question, P. Allemand and collaborators recently implemented the survey of a river located on Basse-Terre Island (Guadeloupe archipelago). Their preliminary observations reveal that the cobbles deposited at the end of a flood are the first entrained at the beginning of the next (P. Allemand, personal communication, 30 June 2017). Based on this observation, we speculate that a tracer belonging to the bed load layer at the end of a flood will still be part of the bed load layer at the beginning of the next one. Similarly, a tracer locked in the bed at the end of a flood will belong to the static layer at the beginning of the next one. In other words, we assume that tracers freeze between two floods.

If this assumption holds, the simplest way to account for bed load intermittency is to assume that the river alternates between two representative stages: (1) a low-flow stage during which tracers are immobile and (2) a flood stage characterized by a representative sediment flux $q_s \sim \alpha V/d_s^2$ during which tracers propagate downstream (Paola et al., 1992; Phillips et al., 2013). Following this model, we may extrapolate our results to the field, provided we rescale time with respect to an intermittency factor $I = T_e/T$, where T is the total duration of elapsed time, and T_e is the time during which sediments are effectively in motion (Paola et al., 1992; Parker et al., 1998; Phillips et al., 2013).

In practice, evaluating the intermittency factor requires continuous monitoring of the river discharge and a correct estimate of the entrainment threshold. Liébault et al. (2012), for instance, monitored the location of tracer cobbles deposited in the Bouinenc stream (France) during 2 years. Over this period, the motion of the tracers resulted from 55 floods for a total duration of 42 days. Sediments were thus in motion less than $I = 12\,\%$ of the time.

Here, we suggest another way to circumvent the intermittency of sediment transport. Plotting the plume variance, $(\sigma^2 - \sigma_0^2)$, and its skewness, γ, as a function of traveled distance, $\langle x\rangle - \langle x\rangle_0$, eliminates time from the equations (Fig. 4). In this plot, the position of the plume acts as a proxy for the effective duration of sediment transport, T_e. The resulting curves are thus filtered from transport intermittency (Fig. 4).

The entrainment regime corresponds to small traveled distances. In this regime, both the size of the plume and its asymmetry increase with traveled distance (Fig. 4). Equations (39), (40), and (41) describe the early evolution of the plume. Eliminating time by combining them, we find the behavior of the plume for short traveled distances:

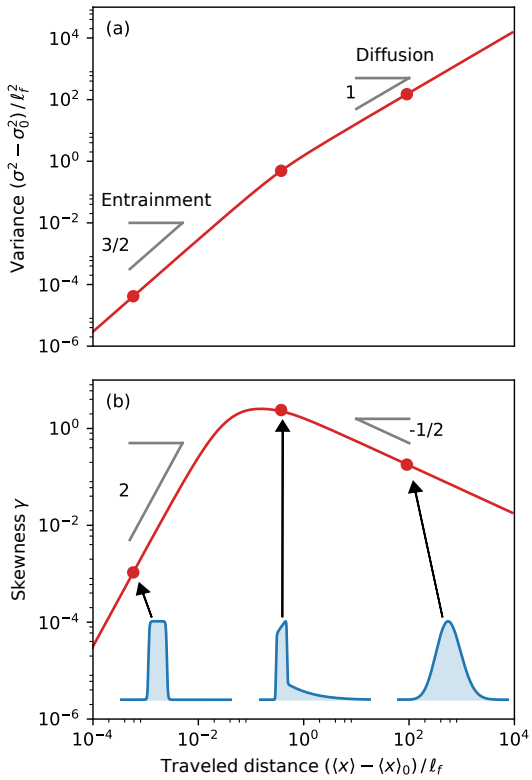

Figure 4. **(a)** Variance and **(b)** skewness of a plume of tracers as a function of traveled distance ($\alpha = 0.1$). These three quantities are calculated from Eqs. (28), (33), and (38). Inset: concentration profiles (blue) illustrating the shape of the plume during the entrainment regime (left), at the transition between the entrainment and the diffusive regime (center), and in the diffusive regime (right).

$$\sigma^2 - \sigma_0^2 = \sqrt{\frac{8\ell_f}{9\alpha}}(\langle x\rangle - \langle x\rangle_0)^{3/2}, \tag{46}$$

$$\gamma = \frac{\ell_f}{\alpha\sigma_0^3}(\langle x\rangle - \langle x\rangle_0)^2. \tag{47}$$

As discussed in Sect. 5, these scalings result from the gradual entrainment of the tracers that are initially trapped in the bed.

After the plume has traveled over a distance roughly equal to the flight length, its skewness reaches a maximum value and starts decreasing. This change in dynamics indicates the transition towards the diffusive regime. Equations (42), (43), and (44) provide the long-term behavior of the plume:

$$\sigma^2 - \sigma_0^2 \sim 2\ell_f(\langle x\rangle - \langle x\rangle_0), \tag{48}$$

$$\gamma = \frac{3}{\sqrt{2}}\sqrt{\frac{\ell_f}{\langle x\rangle - \langle x\rangle_0}}. \tag{49}$$

The linear increase in the variance with the distance traveled by the plume is the signature of standard diffusion (see Sect. 5).

Equating the skewness estimated from Eqs. (47) and (49) provides the position $\langle x\rangle_{\max}$ at which the skewness reaches its maximum:

$$\langle x\rangle_{\max} - \langle x\rangle_0 \sim \left(\frac{3\alpha}{\sqrt{2}}\right)^{2/5}\left(\frac{\sigma_0^6}{\ell_{\mathrm{f}}}\right)^{1/5}. \tag{50}$$

The entrainment regime lasts until the plume has traveled over a distance comparable to its initial size, which is until $\langle x\rangle - \langle x\rangle_0 \sim \sigma_0$.

When expressed in terms of the distance traveled by the plume, the asymptotic regimes are insensitive to the intermittency of bed load transport. They are thus a robust test of our model and can help us interpret field data. Let us assume that a dataset records the evolution of a plume of tracers released in a river over a distance long enough to explore both the entrainment and the diffusive regime. During the diffusive regime, the skewness decreases with the traveled distance. A fit of the data with Eq. (49) yields the flight length, ℓ_{f}. Knowing the latter, we could use Eq. (47) to estimate the intensity of sediment transport, α, from the evolution of the skewness during the entrainment regime.

According to Sect. 5, the skewness reaches a maximum after a time τ_{e} (Eq. 45). Taking into account the intermittency of bed load transport in natural streams, we expect that this maximum is reached when

$$t = (72)^{1/9}\left(\frac{\sigma_0^2}{\alpha}\right)^{1/3}\frac{\tau_{\mathrm{f}}}{I}, \tag{51}$$

where I is the intermittency factor. Identifying this maximum in a field experiment thus yields the ratio τ_{f}/I. Combining the latter with our estimates of the flight length, ℓ_{f}, and the intensity of sediment transport, α, should provide us with the average sediment transport rate in the river:

$$\overline{q_{\mathrm{s}}} = I\alpha d_{\mathrm{s}}^2\frac{l_{\mathrm{f}}}{\tau_{\mathrm{f}}}. \tag{52}$$

7 Conclusion

We used the erosion–deposition model introduced by Charru et al. (2004) to describe the evolution of a plume of bed load tracers entrained by a steady flow. In this model, the propagation of the plume results from the stochastic exchange of particles between the bed and the bed load layer. This mechanism is reminiscent of the propagation of tracers in a porous medium (Berkowitz and Scher, 1998). The evolution of the plume depends on two control parameters: its initial size, σ_0, and the intensity of sediment transport, α.

Our model captures in a single theoretical framework the transition between two asymptotic regimes: (1) an early entrainment regime during which the plume spreads nonlinearly and (2) a late-time relaxation towards classical advection–diffusion. The latter regime is consistent with previous observations (Nikora et al., 2002; Zhang et al., 2012).

When expressed in terms of the distance traveled by the plume, the asymptotic regimes are insensitive to the intermittency of bed load transport in natural streams. According to this model, it should be possible to estimate the particle flight length and the average bed load transport rate from the evolution of the variance and the skewness of a plume of tracers in a river.

Data availability. No data sets were used in this article.

Competing interests. The authors declare that they have no conflict of interest.

Acknowledgements. It is our pleasure to thank Pascal Allemand, David John Furbish, Colin Phillips, Douglas Jerolmack, and François Métivier for many helpful and enjoyable discussions. This work was supported by the French national program EC2CO-Biohefect/Ecodyn//Dril/MicrobiEn, "Dispersion de contaminants solides dans le lit d'une rivire".

Edited by: Patricia Wiberg
Reviewed by: two anonymous referees

References

Agudo, J. and Wierschem, A.: Incipient motion of a single particle on regular substrates in laminar shear flow, Phys. Fluids, 24, 093302, https//doi.org/10.1063/1.4753941, 2012.

Ancey, C., Davison, A., Bohm, T., Jodeau, M., and Frey, P.: Entrainment and motion of coarse particles in a shallow water stream down a steep slope, J. Fluid Mech., 595, 83–114, https://doi.org/10.1017/S0022112007008774, 2008.

Berkowitz, B. and Scher, H.: Theory of anomalous chemical transport in random fracture networks, Phys. Rev. E, 57, 5858, https://doi.org/10.1103/PhysRevE.57.5858, 1998.

Blom, A. and Parker, G.: Vertical sorting and the morphodynamics of bed form–dominated rivers: A modeling framework, J. Geophys. Res.-Ea. Surf., 109, F02007, https://doi.org/10.1029/2003JF000069, 2004.

Bradley, D. N.: Direct Observation of Heavy-Tailed Storage Times of Bed Load Tracer Particles Causing Anomalous Superdiffusion, Geophys. Res. Lett., 44, 12227–12235, https://doi.org/10.1002/2017GL075045, 2017.

Bradley, D. N. and Tucker, G. E.: Measuring gravel transport and dispersion in a mountain river using passive radio tracers, Earth Surf. Proc. Land., 37, 1034–1045, 2012.

Bradley, D. N., Tucker, G. E., and Benson, D. A.: Fractional dispersion in a sand bed river, J. Geophys. Res., 115, F00A09, https://doi.org/10.1029/2009JF001268, 2010.

Charru, F.: Selection of the ripple length on a granular bed sheared by a liquid flow, Phys. Fluids, 18, 121508-1–121508-9, https://doi.org/10.1017/S002211200500786X, 2006.

Charru, F., Mouilleron, H., and Eiff, O.: Erosion and deposition of particles on a bed sheared by a viscous flow, J. Fluid Mech., 519, 55–80, 2004.

Crickmore, M. and Lean, G.: The measurement of sand transport by means of radioactive tracers, in: P. Roy. Soc. Lond. A, 266, 402–421, 1962.

Einstein, H. A.: Bed load transport as a probability problem, in: Sedimentation: 746 Symposium to Honor Professor H. A. Einstein, 1972 (translation from 747 German of H. A. Einstein doctoral thesis), Originally presented to Federal Institute of Technology, Zurich, Switzerland, C1–C105, 1937.

Fathel, S., Furbish, D., and Schmeeckle, M.: Parsing anomalous versus normal diffusive behavior of bed load sediment particles, Earth Surf. Proc. Land., 41, 1797–1803, https://doi.org/10.1002/esp.3994, 2016.

Fernandez-Luque, R. and Van Beek, R.: Erosion and transport of bed-load sediment, J. Hydraul. Res., 14, 127–144, 1976.

Furbish, D. J., Ball, A., and Schmeeckle, M.: A probabilistic description of the bed load sediment flux: 4. Fickian diffusion at low transport rates, J. Geophys. Res., 117, F03034, https://doi.org/10.1029/2012JF002356, 2012a.

Furbish, D. J., Haff, P., Roseberry, J., and Schmeeckle, M.: A probabilistic description of the bed load sediment flux: 1. Theory, J. Geophys. Res., 117, F03031, https://doi.org/10.1029/2012JF002352, 2012b.

Furbish, D. J., Roseberry, J., and Schmeeckle, M.: A probabilistic description of the bed load sediment flux: 3. The particle velocity distribution and the diffusive flux, J. Geophys. Res., 117, F03033, https://doi.org/10.1029/2012JF002355, 2012c.

Furbish, D. J., Fathel, S. L., Schmeeckle, M. W., Jerolmack, D. J., and Schumer, R.: The elements and richness of particle diffusion during sediment transport at small timescales, Earth Surf. Proc. Land., 42, 214–237, https://doi.org/10.1002/esp.4084, 2017.

Ganti, V., Meerschaert, M. M., Foufoula-Georgiou, E., Viparelli, E., and Parker, G.: Normal and anomalous diffusion of gravel tracer particles in rivers, J. Geophys. Res.-Ea. Surf., 115, doi:10.1029/2008JF001222, 2010.

Gintz, D., Hassan, M. A., and SCHMIDT, K.-H.: Frequency and magnitude of bedload transport in a mountain river, Earth Surf. Proc. Land., 21, 433–445, 1996.

Hassan, M. A., Voepel, H., Schumer, R., Parker, G., and Fraccarollo, L.: Displacement characteristics of coarse fluvial bed sediment, J. Geophys. Res.-Ea. Surf., 118, 155–165, 2013.

Helley, E. J. and Smith, W.: Development and calibration of a pressure-difference bedload sampler, US Geol. Survey Open-File Report, USGS, Washington, DC, 1971.

Houssais, M. and Lajeunesse, E.: Bedload transport of a bimodal sediment bed, J. Geophys. Res.-Ea. Surf., 117, F04015, doi:10.1029/2012JF002490, 2012.

James, F., Postel, M., and Sepúlveda, M.: Numerical comparison between relaxation and nonlinear equilibrium models. Application to chemical engineering, Physica D, 138, 316–333, 2000.

Lajeunesse, E., Malverti, L., and Charru, F.: Bedload transport in turbulent flow at the grain scale: experiments and modeling, J. Geophys. Res.-Ea. Surf., 115, F04001, https://doi.org/10.1029/2009JF001628, 2010a.

Lajeunesse, E., Malverti, L., and Charru, F.: Bedload transport in turbulent flow at the grain scale: experiments and modeling, J. Geophys. Res, 115, F04001, https://doi.org/10.1029/2009JF001628, 2010b.

Lajeunesse, E., Devauchelle, O., Houssais, M., and Seizilles, G.: Tracer dispersion in bedload transport, Adv. Geosci., 37, 1–6, https://doi.org/10.5194/adgeo-37-1-2013, 2013.

Lajeunesse, E., Devauchelle, O., Lachaussée, F., and Claudin, P.: Bedload transport in laboratory rivers: the erosion-deposition model, in: Gravel-bed Rivers: Gravel Bed Rivers and Disasters, Wiley-Blackwell, Oxford, UK, 415–438, 2017.

Lenzi, M., Mao, L., and Comiti, F.: Magnitude-frequency analysis of bed load data in an Alpine boulder bed stream, Water Resour. Res., 40, W07201, doi:10.1029/2003WR002961, 2004.

Leopold, L. B. and Emmett, W. W.: Bedload measurements, East Fork River, Wyoming, P. Natl. Acad. Sci. USA, 73, 1000–1004, 1976.

Liébault, F., Bellot, H., Chapuis, M., Klotz, S., and Deschâtres, M.: Bedload tracing in a high-sediment-load mountain stream, Earth Surf. Proc. Land., 37, 385–399, 2012.

Liu, Y., Metivier, F., Lajeunesse, E., Lancien, P., Narteau, C., and Meunier, P.: Measuring bed load in gravel bed mountain rivers : averaging methods and sampling strategies, Geodynamica Acta, 21, 81–92, https://doi.org/10.3166/ga.21.81-92, 2008.

Martin, R. L., Jerolmack, D. J., and Schumer, R.: The physical basis for anomalous diffusion in bed load transport, J. Geophys. Res., 117, F01018, https://doi.org/10.1029/2011JF002075, 2012.

Nikora, V., Habersack, H., Huber, T., and McEwan, I.: On bed particle diffusion in gravel bed flows under weak bed load transport, Water Resour. Res., 38, 1081, https://doi.org/10.1029/2001WR000513, 2002.

Nino, Y. and Garcia, M.: Gravel saltation. Part I: Experiments, Water Resour. Res., 30, 1907–1914, 1994.

Paola, C., Hellert, P., and Angevine, C.: The large-scale dynamics of grain-size variation in alluvial basins, 1: theory, Basin Res., 4, 73–90, 1992.

Parker, G., Paola, C., Whipple, K., Mohrig, D., Toro-Escobar, C., Halverson, M., and Skoglund, T.: Alluvial fans formed by channelized fluvial and sheet flow. II: Application, J. Hydraul. Eng., 124, 996–1004, 1998.

Pelosi, A., Parker, G., Schumer, R., and Ma, H.-B.: Exner-Based Master Equation for transport and dispersion of river pebble tracers: Derivation, asymptotic forms, and quantification of nonlocal vertical dispersion, J. Geophys. Res.-Ea. Surf., 119, 1818–1832, 2014.

Phillips, C. B. and Jerolmack, D.: Dynamics and mechanics of bedload tracer particles, Earth Surf. Dynam., 2, 513–530, 2014.

Phillips, C. B. and Jerolmack, D. J.: Self-organization of river channels as a critical filter on climate signals, Science, 352, 694–697, 2016.

Phillips, C. B., Martin, R. L., and Jerolmack, D. J.: Impulse framework for unsteady flows reveals superdiffusive bed load transport, Geophys. Res. Lett., 40, 1328–1333, 2013.

Roseberry, J., Schmeeckle, M., and Furbish, D.: A probabilistic description of the bed load sediment flux: 2. Particle activity and motions, J. Geophys. Res., 117, F03032, https://doi.org/10.1029/2012JF002353, 2012.

Sayre, W. and Hubbell, D.: Transport and dispersion of labeled bed material, North Loup River, Nebraska, Tech. Rep. 433-C, US Geol. Surv. Prof. Pap., US Geological Survey, United-States Governement Printing Office, Washington, 1965.

Schumer, R., Meerschaert, M. M., and Baeumer, B.: Fractional advection-dispersion equations for modeling transport at the Earth surface, J. Geophys. Res.-Ea. Surf., 114, F00A07, doi:10.1029/2008JF001246, 2009.

Seizilles, G., Lajeunesse, E., Devauchelle, O., and Bak, M.: Cross-stream diffusion in bedload transport, Phys. Fluids, 26, 013302, https://doi.org/10.1063/1.4861001, 2014.

Shields, A. S.: Anwendung der Aehnlichkeitsmechanik und der Turbulenzforschung auf die Geschiebebewegung, Mitteilung der Preussischen Versuchsanstalt fur Wasserbau und Schiffbau, 26, 524–526, 1936.

Taylor, G.: Dispersion of soluble matter in solvent flowing slowly through a tube, P. Roy. Soc Lond. A, 219, 186–203, 1953.

Turowski, J. M., Yager, E. M., Badoux, A., Rickenmann, D., and Molnar, P.: The impact of exceptional events on erosion, bedload transport and channel stability in a step-pool channel, Earth Surf. Proc. Land., 34, 1661–1673, 2009.

Turowski, J. M., Badoux, A., and Rickenmann, D.: Start and end of bedload transport in gravel-bed streams, Geophys. Res. Lett., 38, L04401, doi:10.1029/2010GL046558, 2011.

Van Genuchten, M. T. and Wierenga, P.: Mass transfer studies in sorbing porous media I. Analytical solutions, Soil Sci. Soc. Am. J., 40, 473–480, 1976.

Van Rijn, L.: Sediment transport, part I: bed load transport, J. Hydrual. Eng., 110, 1431–1456, 1984.

Weeks, E. R. and Swinney, H. L.: Anomalous diffusion resulting from strongly asymmetric random walks, Phys. Rev. E, 57, 4915–4920, doi:10.1103/PhysRevE.57.4915, 1998.

Zhang, Y., Meerschaert, M. M., and Packman, A. I.: Linking fluvial bed sediment transport across scales, Geophys. Res. Lett., 39, L20404, doi:10.1029/2012GL053476, 2012.